

ProFound: A moderate-sized vision foundation model for multi-task prostate imaging

Yipei Wang^{1,2}[0000-0002-9589-7177], Yinsong Xu^{1,3}[0000-0002-1050-0143], Weixi Yi^{1,2}[0009-0002-9889-9853], Shaheer Ullah Saeed^{1,2,4,5,6}[0000-0002-5004-0663], Natasha Thorley^{7,8}[0000-0001-8928-895X], Alexander Ng^{9,12}[0000-0001-5441-2017], Yukun Zhou^{1,10}[0000-0002-0840-6422], Wen Yan^{1,2}[0000-0002-3962-5994], Dean Barratt^{1,2}[0000-0003-2916-655X], Shonit Punwani^{7,8}[0000-0002-1014-0870], Veeru Kasivisvanathan^{9,11,12,13}[0000-0002-0832-382X], Mark Emberton^{11,12}[0000-0003-4230-0338], Daniel C. Alexander^{1,14}[0000-0003-2439-350X], and Yipeng Hu^{1,2}[0000-0003-4902-0486]

¹ UCL Hawkes Institute, University College London, London, UK
yipei.wang@ucl.ac.uk

² Department of Medical Physics and Biomedical Engineering, University College London, London, UK

³ School of Artificial Intelligence, Beijing University of Posts and Telecommunications, Beijing, China

⁴ Centre for Bioengineering, Queen Mary University of London, London, UK

⁵ School of Engineering and Materials Science, Queen Mary University of London, London, UK

⁶ Digital Environment Research Institute, Queen Mary University of London, London, UK

⁷ Centre for Medical Imaging, University College London, London, UK

⁸ Department of Radiology, University College London Hospital NHS Foundation Trust, London, UK

⁹ Centre for Urology Imaging, Prostate, AI and Surgical Studies (COMPASS) Research Group, Division of Surgery and Interventional Science, University College London, London, UK

¹⁰ Institute of Ophthalmology, University College London, London, UK

¹¹ Department of Urology, University College London Hospital, London, UK

¹² Division of Surgery and Interventional Science, University College London, London, UK

¹³ Department of Urology, Comprehensive Cancer Center, Medical University of Vienna, Vienna, Austria

¹⁴ Department of Computer Science, University College London, London, UK

Abstract. Many diagnostic and therapeutic clinical tasks for prostate cancer increasingly rely on multi-parametric MRI. Automating these tasks is challenging because they necessitate expert interpretations, which are difficult to scale to capitalise on modern deep learning. Although modern automated systems achieve expert-level performance in isolated tasks, their general clinical utility remains limited by the requirement of large task-specific labelled datasets. In this paper, we present ProFound, a domain-specialised vision foundation model for volumetric prostate mpMRI. ProFound is pre-trained using several variants of self-supervised

approaches on a diverse, multi-institutional collection of 5,000 patients, with a total of over 22,000 unique 3D MRI volumes (over 1,800,000 2D image slices). We conducted a systematic evaluation of ProFound across a broad spectrum of 11 downstream clinical tasks on over 3,000 independent patients, including prostate cancer detection, Gleason grading, lesion localisation, gland volume estimation, zonal and surrounding structure segmentation. Experimental results demonstrate that finetuned ProFound consistently outperforms or remains competitive with state-of-the-art specialised models and existing medical vision foundation models trained/finetuned on the same data. In this paper, we share real-world experience in developing and assessing ProFound, with a set of rigorous, large-scale clinical evaluations. To facilitate deployment and finetuning under heterogeneous clinical compute constraints, we adopt a moderate-sized, efficient architecture. ProFound offers a scalable framework for advancing compute-and-data efficiency in prostate oncology. All model weights, implementation as well as an interactive interface are publicly available at <https://github.com/pipiwang/ProFound> and <https://huggingface.co/spaces/Anonymise/ProFound>.

Keywords: Prostate Cancer · mpMRI · Foundation model.

1 Introduction

Prostate cancer remains one of the leading causes of cancer-related mortality in men, and early, accurate diagnosis is crucial for improving patient outcomes. In current clinical pathways, multi-parametric MRI (mpMRI) is increasingly used across multiple stages of care, including pre-biopsy risk stratification, lesion targeting, and surgical and radiotherapy planning. Interpretation of mpMRI and the associated downstream decisions remain highly dependent on expert radiological assessment, which can introduce variability in reporting. In this context, deep learning for prostate MRI has shown progress in several clinical tasks, including cancer detection/classification and lesion or anatomy segmentation [25, 27, 14]. However, automation using deep learning often requires a large volume of labelled data, which becomes increasingly infeasible for wider adoption in different centres and for diverging tasks.

General-purpose radiology foundation models aim to reduce the data requirements for specific downstream tasks by providing an easy-to-generalise model trained across many organs and modalities [22, 28] and have shown potential in achieving better performance for individual applications. However, achieving strong performance often still requires substantially larger amounts of pretraining data, even millions [22]. In addition, for tasks involving prostate MR, model performance remains insufficient for clinical use due to the under-representation of prostate mpMRI, likely because prostate mpMRI is a highly specialised multi-sequence protocol and its widespread standardisation in clinical practice (e.g., through PI-RADS [17]) is relatively new.

Recent efforts have begun to explore domain-specialised foundation models for prostate imaging. ProViCNet [7] introduced a prostate-specific vision

transformer for clinically significant cancer detection on mpMRI and TRUS, leveraging patch-level contrastive learning to enhance lesion discrimination and demonstrating strong detection performance. ProstNFound [20] adapted medical foundation models to micro-ultrasound by incorporating domain-specific texture prompts and clinical metadata, achieving competitive ultrasound-based cancer detection performance and highlighting the importance of injecting modality-specific priors into foundation models. Despite these advances, existing approaches remain largely task-centric and/or modality-specific, focusing on a diagnostic objective (primarily cancer detection) rather than learning a unified prostate representation that can transfer across the broader set of clinical tasks required in prostate cancer management. In practice, beyond cancer detection, mpMRI has an arguably wider range of clinical applications, including lesion delineation for therapy planning, localisation at clinically actionable region levels, grading/risk stratification, etc. A prostate-dedicated, volumetric foundation model trained directly on large-scale prostate mpMRI and evaluated systematically across these diverse downstream tasks remains unexplored.

To examine whether a practically feasible pretraining data scale can still support broad downstream utility, we present ProFound, a vision foundation model pre-trained using self-supervised masked autoencoding [5] on a moderate-scale, multi-institutional collection of prostate mpMRI data drawn from diverse patient populations and clinical cohorts (e.g., screening, diagnostic, and treatment-planning pathways) and using T2w, DWI, and ADC sequences to learn prostate-specific volumetric representations. We evaluate ProFound across multiple downstream clinical tasks spanning classification, segmentation, localisation, and regression, and compare against (i) task-specific models trained from scratch and (ii) existing generalist medical foundation models as well as general vision pretraining baselines. Further, we study ProFound’s efficiency under limited available finetuning data and limited finetuning regimes, and report systematic clinical evaluation including comparisons to radiologist performance and histopathology reference standard. Integrating deep learning into real-world clinical workflows requires models that can run efficiently and securely on standard hospital hardware without prohibitive computational costs. These have motivated our moderately-sized, efficient, and open-source ProFound, for a scalable framework for compute- and data-efficient prostate imaging analysis. ProFound is open-sourced at <https://github.com/pipiwang/ProFound>.

2 Method

2.1 Data

Pretrain dataset ProFound is pretrained on a large and diverse collection of prostate MRIs aggregated from multiple datasets, including two public datasets: the PICAI challenge dataset [13] and the Cancer Imaging Archive (TCIA) dataset [2], comprising 1,500 and 863 patients respectively; and two private datasets: the ReIMAGINE Risk study dataset [9] with 491 patients and a multi-institute

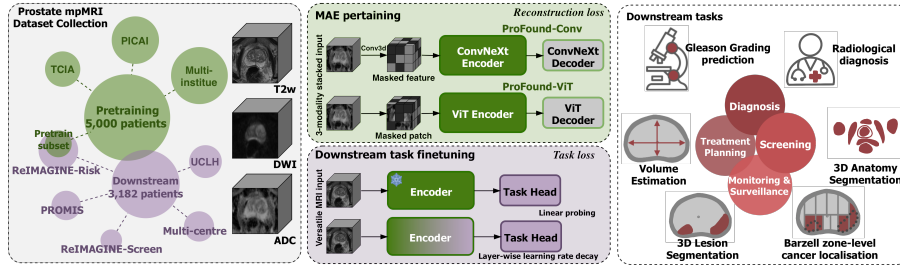


Fig. 1. Overview of the proposed prostate mpMRI foundation model.

dataset [11] with 2,146 patients. Three MRI modalities were used during pre-training, including T2-weighted (T2w), high b-value diffusion-weighted (DWI) and apparent diffusion coefficient (ADC) MRI. The number of available mpMRI scans varied across patients, ranging from 1 to 28 three-modality triplets per patient, resulting in a total of 8,893 pretraining triplets from 5,000 patients. All images were resampled to an isotropic spatial resolution of $1mm \times 1mm \times 1mm$, spatially aligned across modalities, and intensity-normalised to a consistent range. We applied data augmentation consisting of random isotropic zooming, random spatial cropping, and random flipping along the axial axis.

Downstream task finetuning and evaluation dataset Various downstream tasks were performed on the following prostate mpMRI datasets: the multi-institute ReIMAGINE Risk from 1,028 patients [9], the ReIMAGINE Screen dataset from 304 patients [10], the PROMIS study dataset from 566 patients [19], the UCLH dataset from 695 patients [26], and a multi-centre pelvis MR dataset with 589 patients [8]. All datasets were divided into finetuning/training, validation and test sets in a 7:1:2 ratio. The downstream task datasets follow the same preprocessing pipeline as the pretraining dataset.

2.2 Pretraining

In this work, we adopt the masked autoencoder (MAE) [5] framework to pre-train large-scale volumetric foundation models using two variants under a unified self-supervised objective. Given a combination of T2w, high-b DWI, and ADC from one patient, the 3D mpMRI sequences are stacked as channels to form a 3-modality input. A high proportion of patches or image volumes are masked to train the network to reconstruct the missing content from the remaining visible context. We investigate two 3D masked autoencoder architectures: 1) **ProFound-ViT** is a ViT-based 3D MAE adapted from ViT-B [3]. It tokenises the 3D volumes into non-overlapping cubic patches, processes visible patches with Transformer blocks using fixed 3D sine-cosine positional embeddings, and reconstructs masked patches with a lightweight decoder following the standard asymmetric MAE design. The reconstruction loss is computed only over the masked image volumes; 2) **ProFound-Conv** is a fully convolutional 3D MAE

Table 1. Description of ProFound downstream tasks and extended analysis. Cat. = Category, Cls = classification, Seg = segmentation, Reg = regression, Loc = localisation, mul = multi-class, bin = binary, GG = Gleason group, FM = Foundation model

Task name	Description	Dataset	Subtask	Cat.
PIRADS-Cls	Automating radiologist task by predicting PIRADS score	ReIMAGINE-Risk	PIRADS $\leq 3, 3, 4, 5$	mul-Cls
			PIRADS < 3 vs. ≥ 3	bin-Cls
			PIRADS ≤ 3 vs. > 3	bin-Cls
Grading-Cls	Predicting Gleason Grade Group on patients with MR-positive lesions	PROMIS	GG $\leq 6, 3+4, 4+3, 8, > 8$	mul-Cls
			GG $\leq 3 + 4$ vs. ≤ 6	bin-Cls
			GG $\leq 4 + 3$ vs. $\leq 3 + 4$	bin-Cls
LesionSegAll	Delineating lesion contour on all patients	UCLH		bin-Seg
LesionSegRad	Delineating lesion contour on radiology-positives	PROMIS (PIRADS > 2 subset)		bin-Seg
AnatomySeg	Multi-structure segmentation for focal therapy	multi-centre		mul-Seg
Volume-Reg	Prostate volume estimation	UCLH		Reg
PCa-Loc	Histopathological PCa detection on Barzell zones	PROMIS		Loc
Tang et al[16]	Impact of image quality on FM finetuning	PRIME		
Sidiqi et al[15]	Investigating task-aligned continual pretraining	PROMIS, UCLH, ReIMAGINE-Risk		
Huang et al[6]	Studying task alignment and transferability	PROMIS, multi-centre		
Wang et al[18]	Interpreting downstream task finetuning	UCLH, ReIMAGINE-Risk		

based on ConvNeXtV2 [21]. Rather than tokenising patches, it preserves a dense 3D feature grid and applies masking directly in the spatial domain. The encoder uses sparse convolutions to operate primarily on visible voxels for improved efficiency, while a lightweight convolutional decoder restores masked regions using learned mask tokens. The reconstruction loss is applied only to masked regions.

2.3 Downstream task finetuning

A wide range of downstream tasks were chosen as described in Tab 1. For classification, we use two fully connected layers with an intermediate batch normalisation layer. For segmentation, we assess two commonly used architectures, UperNet [24] and UNetR3D [4]. For AnatomySeg, ProFound is adapted to take only T2w by zeroing out the other two input channels. The localisation task predicts cancer presence on Barzell zones of the prostate [23], which follows the same design as the segmentation task (UNetR3D), with an additional layer that performs zone-wise feature aggregation and subsequent classification. For regression, we adopt a batch normalisation layer followed by a fully connected layer.

2.4 Experiments for evaluating downstream tasks

To assess the impact of prostate-specific pretraining and data efficiency, we evaluate ProFound against three categories of models and various adaptation regimes: **Foundation Model Baselines:** We compare against RadFM [22] (pretrained on 16M radiological pairs), RadDiag [28] (pretrained on 192k multi-modal scans), and a DINOv2 [12] baseline trained on our pretrain dataset to isolate the effects of the MAE objective and architecture.

Specialised Models: To quantify pretraining advantages, ProFound backbones (ViT and ConvNeXtV2) are compared against identical architectures trained

from scratch and standard 3D medical imaging baselines: ResNet18 (Cls/Reg tasks) and UNet (Seg/Loc tasks) using the same data for finetuning.

Adaptation Strategies: We evaluate two regimes: linear probing (frozen encoder) and full finetuning using layer-wise learning rate decay (LLRD) for stable feature preservation.

Data Efficiency: Models are tested under constrained conditions (8 to 128 samples) to simulate clinical scenarios where annotations are scarce.

Evaluation Metrics: Performance is averaged across three runs. For ordinal multi-class tasks, we use Quadratic Weighted Kappa and binary AUC (with sensitivity/specificity at 80% fixed operating points). Segmentation is evaluated via the Dice score, and volume estimation via Mean Absolute Error (MAE). Statistical significance is determined using paired t-tests.

Implementation: The mask ratios for ProFound-ViT and ProFound-Conv during pretraining were set to 0.75 and 0.6, respectively, following [5] and [21]. The best performing model is selected based on the validation set evaluation within 100 epochs of finetuning or training. The classification, segmentation, and regression tasks are trained using cross-entropy loss, Dice with cross-entropy loss, and Mean Squared Error loss respectively. Note that in less data settings, UNet is unstable when trained with Dice with cross-entropy loss, therefore all comparison models are trained with Dice loss. ProFound-ViT and ProFound-Conv are pretrained on 4 RTX8000 GPUs for 10 days and 4 A6000 GPUs for 14 days respectively. Further implementation details including pretrain/finetune epochs, learning rates, etc., can be found in the open-source repository.

3 Results

ProFound achieves SOTA performance in segmentation tasks: For prostate lesion segmentation on all patients with MRI scans, ProFound-Conv achieves the best performance with a Dice of (0.429 ± 0.009) , significantly outperforming the strongest specialised baseline UNet $(0.416 \pm 0.004, p = 0.001)$. Overall, models leveraging foundation pretraining tend to outperform their train-from-scratch counterparts, highlighting the value of large-scale pretraining for prostate MRI representation learning. Notably, ProFound-Conv also significantly exceeds DINOv2 $(0.415 \pm 0.007, p < 0.0001)$, despite DINOv2 being pretrained on the same dataset as ProFound.

For lesion segmentation on radiologist-positive patients, Dice scores decrease across all methods. This could partially be attributed to the smaller dataset size and that the UCLH dataset is specifically collected for patients enrolled in focal therapy, which are expected to include larger and more conspicuous lesions, while the PROMIS dataset is collected on a biopsy-blind diagnostic cohort. Nonetheless, ProFound-Conv with frozen encoder ranks highest (0.297 ± 0.005) , closely followed by other ProFound variants $(0.296 \pm 0.009$ and $0.293 \pm 0.008)$.

For the prostate anatomy segmentation task, ProFound-ViT with fixed encoder achieves the top Dice of 0.931 ± 0.001 , significantly outperforming Rad-Diag (0.921 ± 0.001) . Across segmentation tasks, ProFound models with UN-

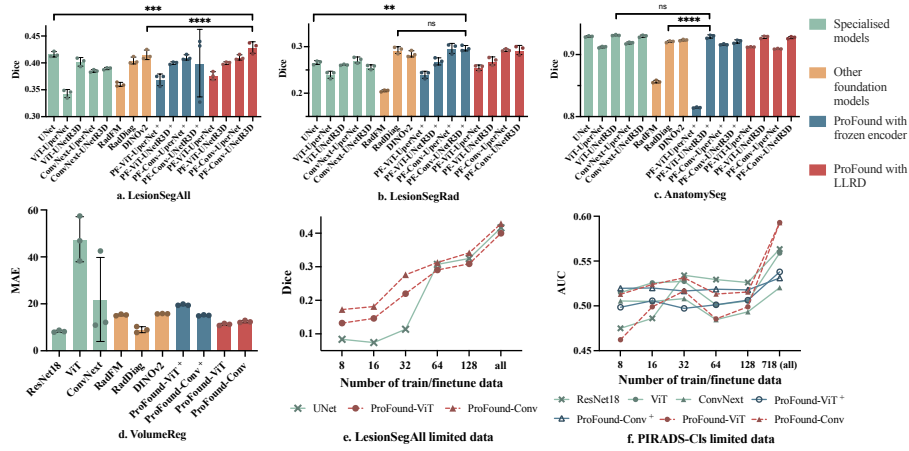


Fig. 2. Performance on representative downstream tasks. ProFound achieves the highest Dice scores on both lesion segmentation tasks, while remaining comparable to SOTA specialised models on anatomy segmentation and prostate volume regression. ProFound shows a clear advantage in limited-label settings, demonstrating strong data efficiency. We also include a challenging task where ProFound provides more nuanced gains.

etR3D head generally outperform those using UperNet, with all $p < 0.0001$ for LesionSegAll and AnatomySeg tasks (except for ProFound-ViT-UNetR3D on AnatomySeg).

ProFound demonstrates strong data efficiency. In limited-data experiment, ProFound achieves a Dice score of 0.276 with only 32 finetuning cases, and consistently outperforms UNet across all low-data settings, as shown in Fig 2.

ProFound supports prostate cancer detection: For PIRADS score prediction, ProFound-Conv achieved the strongest ordinal agreement with the ground truth (QWK = 0.285), outperforming DINOv2 (0.227), ViT (0.224), and ResNet18 (0.207). Several baselines (e.g., ConvNeXt: 0.010; RadFM :−0.002) demonstrate limited ordinal consistency despite reasonable binary discrimination performance. For binary classification of radiologist-visible cancer (PIRADS ≥ 3 vs. < 3), ProFound-Conv attains the highest AUC (76.1%), followed by ProFound-ViT (75.6%) and RadFM (73.4%). At clinically meaningful operating points, RadFM yields the highest sensitivity at 80% specificity (62.6%), while ProFound-ViT and RadDiag achieve the highest specificity at 80% sensitivity (55.6%).

For Gleason Grading classification among MR-positive patients, ProFound-Conv again provides the best ordinal agreement (QWK = 0.169), followed by RadDiag (0.147) and DINOv2 (0.100). In contrast, multiple supervised baselines exhibited near-zero or negative QWK (e.g., ResNet18: −0.002; ViT: −0.035), indicating poor alignment with grading labels. For binary classification of Gleason Grade Group ≥ 3 , ProFound-Conv achieves the highest AUC (73.5%), surpassing RadDiag (72.0%). At fixed operating points, ProFound-Conv achieves the

highest specificity at 80% sensitivity (60.4%), whereas RadDiag yields the highest sensitivity at 80% specificity (50.4%). As summarised in Table 2, overall, ProFound-Conv offers the most balanced performance across ordinal agreement and binary discrimination.

For Barzell zone-level lesion detection, ProFound-Conv excel in all evaluation metrics, with all ProFound variants improving over both foundation models and supervised models, except for RadDiag which achieves comparable performance. Notably, under the same clinical definition, radiologist readings achieve 39.8% specificity at 80% sensitivity, which is lower than all ProFound variants.

Other results on model interpretability, continual pretraining and further downstream tasks: For prostate volume estimation tasks, ResNet18 achieves the lowest MAE (ml) of 8.28, followed by RadDiag (8.00). ProFound variants show comparable performance of 11.25 and 12.44.

Table 2. Performance comparison for PIRADS score classification, Gleason grade group classification, and localised cancer detection task. Spec = Specificity at 80% sensitivity; Sens = Sensitivity at 80% specificity, + denotes ProFound with frozen encoder (linear probing). The baseline model is ResNet18 for PIRADS-Cls and Grading-Cls tasks, and UNet for the PCa-Loc localisation task. The unit for the number of updated parameters is million.

	PIRADS-Cls				Grading-Cls				Cls	PCa-Loc			Loc
	QWK	AUC	Spec	Sens	QWK	AUC	Spec	Sens	Params	AUC	Spec	Sens	Params
Baseline	0.207	73.2	50.0	49.1	-0.002	59.1	35.4	22.4	33.3	61.3	41.4	25.0	4.8
ViT	0.224	72.1	36.1	56.1	-0.035	47.4	20.8	13.2	123.0	60.5	41.3	26.2	136.3
ConvNeXt	0.010	59.7	38.9	22.2	0.087	59.6	39.6	21.9	29.5	62.4	43.2	30.0	39.5
RadFM	-0.002	73.4	47.2	62.6	0.013	55.7	25.0	18.9	66.4	60.3	38.5	22.7	79.6
RadDiag	0.076	73.3	55.6	54.4	0.147	72.0	47.9	50.4	33.3	63.5	42.7	27.0	119.4
DINOv2	0.227	72.9	44.4	50.9	0.100	60.7	41.7	25.0	92.4	62.1	41.2	28.4	112.7
ProFound-ViT ⁺	0.246	67.4	44.4	43.3	0.035	48.1	31.3	13.6	0.2	63.1	45.4	31.4	13.5
ProFound-Conv ⁺	0.191	50.7	30.6	18.7	0.034	50.6	29.2	15.8	0.2	62.2	43.3	28.7	10.2
ProFound-ViT	0.047	75.6	55.6	58.5	-0.063	49.8	25.0	16.2	123.0	63.1	45.4	31.4	136.3
ProFound-Conv	0.285	76.1	47.2	60.2	0.169	73.5	60.4	49.6	29.5	66.0	46.5	33.4	39.5

The ProFound model was open-sourced prior to writing this report, other studies reported the impact of image quality on ProFound finetuning [16], correlation between pretraining-downstream task alignment and foundation model transferability [6], the effect of continual pretraining on downstream task performance [15], as well as interpreting changes during downstream task finetuning [18]. These developments are not contributions of the present work, however, they provide useful context and offer complementary reference for the results reported in this paper.

4 Discussion and Conclusion

The segmentation results suggest that prostate-specific volumetric pretraining provides consistent gains over both specialised models trained from scratch and generalist foundation models. ProFound outperforms DINOv2 even when pre-trained on the same dataset, indicating that the 3D MAE objective and architectural choices better capture prostate-relevant structure for dense prediction. We also observe that frozen-encoder adaptation can be competitive, particularly in lesion segmentation on smaller cohorts, supporting the practical utility of ProFound in limited label-and-compute finetuning regimes.

Across detection- and grading-based tasks, ProFound-Conv consistently improves ordinal agreement (QWK) while maintaining strong discrimination (AUC), suggesting that prostate-specific volumetric pretraining learns representations aligned with clinically meaningful disease ordering rather than only binary separability. The observation that some generalist models achieve reasonable AUC yet near-zero/negative QWK highlights the importance of evaluating ordinal consistency for PIRADS and Gleason-related endpoints. The improved zone-level localisation relative to radiologist performance suggests ProFound may provide complementary decision support for localised targeting and structured reporting.

A notable strength of this study is the heterogeneity of the multi-centre datasets used for pretraining and downstream evaluation. Cohorts differ in acquisition protocols, scanners, patient selection, and annotation type/quality, introducing realistic domain shift and label noise (e.g., inter-reader variability in lesion boundaries and PI-RADS ratings [1]). ProFound’s consistent performance gains across multiple benchmarks suggest that the learned representations transfer effectively across diverse real-world settings rather than relying on narrowly curated, homogeneous datasets.

This study represents the first version of ProFound, with ongoing development curating larger data sets of higher quality, for pretraining and even broader validation. By fully open-sourcing our open-weight models for specialised clinical needs, this work offers a scalable, data-and compute-efficient foundation to advance the state of the art in prostate oncology.

5 Acknowledgment

This work was supported by the National Institute for Health Research (NIHR) University College London Hospitals (UCLH) Biomedical Research Centre (BRC). This work was also supported by the International Alliance for Cancer Early Detection, an alliance between Cancer Research UK [C28070/A30912; C73666/A31378; EDDAPA-2024/100014], Canary Center at Stanford University, the University of Cambridge, OHSU Knight Cancer Institute, University College London and the University of Manchester.

References

1. Brembilla, G., Dell’Oglio, P., Stabile, A., et al.: Interreader variability in prostate mri reporting using prostate imaging reporting and data system version 2.1. *European radiology* **30**(6), 3383–3392 (2020)
2. Choyke, P., Turkbey, B., Merino, M., Wood, B.: (Jun 2025), <http://doi.org/10.7937/K9/TCIA.2016.6046GUDv>
3. Dosovitskiy, A., Beyer, L., Kolesnikov, A., et al.: An image is worth 16x16 words: Transformers for image recognition at scale. *arXiv preprint arXiv:2010.11929* (2020)
4. Hatamizadeh, A., Tang, Y., Nath, V., et al.: Unetr: Transformers for 3d medical image segmentation. In: *Proceedings of the IEEE/CVF winter conference on applications of computer vision*. pp. 574–584 (2022)
5. He, K., Chen, X., Xie, S., et al.: Masked autoencoders are scalable vision learners. In: *Proceedings of the IEEE/CVF conference on computer vision and pattern recognition*. pp. 16000–16009 (2022)
6. Huang, S., Wang, Y., Thorley, N., et al.: Understanding the transfer limits of vision foundation models. *arXiv preprint arXiv:2601.15888* (2026)
7. Lee, J.H., Li, C.X., Jahanandish, H., et al.: Prostate-specific foundation models for enhanced detection of clinically significant cancer. *arXiv preprint arXiv:2502.00366* (2025)
8. Li, Y., Fu, Y., Gayo, I.J., et al.: Prototypical few-shot segmentation for cross-institution male pelvic structures with spatial registration. *Medical Image Analysis* **90**, 102935 (2023)
9. Marsden, T., Ahmed, H.U., Emberton, M.: An update from the reimagine prostate cancer risk study (nct04060589): A prospective cohort study in men with a suspicion of prostate cancer who are referred onto a magnetic resonance imaging–based diagnostic pathway with donation of tissue, blood, and urine for biomarker analyses. *European Urology* **80**(4), 398–399 (2021)
10. Marsden, T., Lomas, D.J., McCartan, N., et al.: Reimagine prostate cancer screening study: protocol for a single-centre feasibility study inviting men for prostate cancer screening using mri. *BMJ Open* **11**(9) (2021)
11. Min, Z., Bianco, F.J., Yang, Q., et al.: Segmentation versus detection: Development and evaluation of deep learning models for prostate imaging reporting and data system lesions localisation on bi-parametric prostate magnetic resonance imaging. *CAAI Transactions on Intelligence Technology* **10**(3), 689–702 (2025)
12. Oquab, M., Darcet, T., Moutakanni, T., et al.: Dinov2: Learning robust visual features without supervision. *Transactions on Machine Learning Research Journal* (2024)
13. Saha, A., Bosma, J.S., Twilt, J.J., et al.: Artificial intelligence and radiologists in prostate cancer detection on mri (pi-cai): an international, paired, non-inferiority, confirmatory study. *The Lancet Oncology* **25**(7), 879–887 (2024)
14. Sanford, T., Harmon, S.A., Turkbey, E.B., et al.: Deep-learning-based artificial intelligence for pi-rads classification to assist multiparametric prostate mri interpretation: a development study. *Journal of Magnetic Resonance Imaging* **52**(5), 1499–1507 (2020)
15. Sidiqi, B., Wang, Y., U Saeed, S., et al.: Continual pretraining prostate mri vit encoder for task alignment. *IEEE* (2026)
16. Tang, Y., Rajwa, P., Ng, A., et al.: Impact of clinical image quality on efficient foundation model finetuning. In: *International Workshop on Efficient Medical Artificial Intelligence*. pp. 194–204. Springer (2025)

17. Vargas, H., Hötter, A., Goldman, D., et al.: Updated prostate imaging reporting and data system (pirads v2) recommendations for the detection of clinically significant prostate cancer using multiparametric mri: critical evaluation using whole-mount pathology as standard of reference. *European radiology* **26**(6), 1606–1612 (2016)
18. Wang, Y., Chen, Y., Yan, W., et al.: What fine-tuning changes: A radiomic lens on prostate foundation model representations. In: *Medical Imaging with Deep Learning* (2026)
19. Wang, Y., Gayo, I., Thorley, N., et al.: A derived promis data set (Jun 2025), <https://doi.org/10.5281/zenodo.15683922>
20. Wilson, P.F., To, M.N.N., Jamzad, A., et al.: Prostnfound: integrating foundation models with ultrasound domain knowledge and clinical context for robust prostate cancer detection. In: *International conference on medical image computing and computer-assisted intervention*. pp. 499–509. Springer (2024)
21. Woo, S., Debnath, S., Hu, R., et al.: Convnext v2: Co-designing and scaling convnets with masked autoencoders. In: *Proceedings of the IEEE/CVF conference on computer vision and pattern recognition*. pp. 16133–16142 (2023)
22. Wu, C., Zhang, X., Zhang, Y., et al.: Towards generalist foundation model for radiology by leveraging web-scale 2d&3d medical data. *Nature Communications* **16**(1), 7866 (2025)
23. Wu, X., Wang, Y., Yang, Q., et al.: Ai-assisted prostate cancer detection and localisation on biparametric mr by classifying radiologist-positives. In: *Medical Imaging 2025: Computer-Aided Diagnosis*. vol. 13407, pp. 885–890. SPIE (2025)
24. Xiao, T., Liu, Y., Zhou, B., et al.: Unified perceptual parsing for scene understanding. In: *Proceedings of the European conference on computer vision (ECCV)*. pp. 418–434 (2018)
25. Xu, Y., Wang, Y., Shen, Z., et al.: Poisson ordinal network for gleason group estimation using bi-parametric mri. In: *International conference on medical image computing and computer-assisted intervention*. pp. 564–574. Springer Nature Switzerland, Cham (2024)
26. Yan, W., Chiu, B., Shen, Z., et al.: Combiner and hypercombiner networks: Rules to combine multimodality mr images for prostate cancer localisation. *Medical Image Analysis* **91**, 103030 (2024)
27. Yan, W., Hu, Y., Yang, Q., et al.: A semi-supervised prototypical network for prostate lesion segmentation from multimodality mri. *Physics in Medicine & Biology* **70**(8), 085020 (2025)
28. Zheng, Q., Zhao, W., Wu, C., et al.: Large-scale long-tailed disease diagnosis on radiology images. *Nature Communications* **15**(1), 10147 (2024)